ARTICLE

Fourier transform infrared spectroscopy and imaging of dragonfly, damselfly and cicada wing membranes

Mark J. Tobin,[a*] Ljiljana Puskar,[b] Song Ha Nguyen,[c] Jafar Hasan,[d] Hayden K. Webb,[c]
Carol J. Hirschmugl,[e] Michael J. Nasse,[f] Gediminas Gervinskas,[g] Saulius Juodkazis,[g]
Gregory S. Watson,[h] Jolanta A. Watson,[h] David E. Mainwaring,[c] Peter J. Mahon,[c]
Richard Marchant,[i] Russell J. Crawford[c] and Elena P. Ivanova[c]

[a]Infrared Microspectroscopy Beamline, Australian Synchrotron, 800 Blackburn Road, Clayton, Victoria, 3168, Australia
[b]Methods for Material Development, Helmholtz-Zentrum für Materialien und Energie GmbH, 12489 Berlin, Germany
[c]Faculty of Science, Engineering and Technology, Swinburne University of Technology, PO Box 218, Hawthorn, Victoria, 3122, Australia
[d]Indian Institute of Science, Bengaluru, Karnataka, India
[e]Department of Physics, University of Wisconsin–Milwaukee, 1900 E. Kenwood Road, Milwaukee, Wisconsin 53211, USA
[f]Karlsruhe Institute of Technology, Laboratory for Applications of Synchrotron Radiation, Kaiserstr. 12, 76131 Karlsruhe, Germany
[g]Centre for Micro-Photonics, Faculty of Science, Engineering and Technology, Swinburne University of Technology, PO Box 218, Hawthorn, Victoria, 3122, Australia
[h]Faculty of Science, Health, Education and Engineering, University of the Sunshine Coast, Maroochydore DC, Queensland 4558, Australia
[i]Museum Victoria, Melbourne, Victoria, 3001, Australia

Introduction

Insects and plants have evolved highly sophisticated surfaces that provide them with a number of functional advantages for dealing with their environment, and imparting beneficial properties to these organisms.[1] For example, the surface of some leaves, such as those of the lotus plant, are well known to have highly water repellent, or superhydrophobic, properties[2] and this provides the plant with self-cleaning leaf surfaces, benefiting the plant by inhibiting bacterial or fungal infection, or possibly ensuring optimum photosynthetic ability. This is sometimes referred to as the "lotus effect". Similar superhydrophobic behaviour has been observed on insect cuticles, in particular the wings of certain groups such as cicadas, dragonflies and damselflies, where the water repelling properties enable the insects to remain clean and dry in wet and dirty environments.[3–5] Indeed, some insect wing surfaces have recently been shown to have additional antibacterial properties.[6] Such superhydrophobic natural surfaces have attracted the attention of materials scientists for their potential to provide design templates for the development of manufactured materials with similar properties, for applications such as biomedical implants and microfluidic "lab on a chip" devices.[7]

In order to better understand the chemical and topographic properties of these natural surfaces, a range of techniques has been applied in their analysis, including atomic force microscopy (AFM), scanning electron microscopy (SEM) and gas chromatography-mass spectrometry (GC-MS).[4–6,8] The superhydrophobicity, and hence self-cleaning properties, of these surfaces has been shown to arise due to a combination of their surface chemistry and surface topography. In particular, the presence of hierarchical topography, comprising features on the nano- and micro-scale, contributes to their ability to repel water droplets. This, in turn, allows a pristine surface to be maintained by the droplets removing foreign particles as they roll across the surface. A common method for assessing the hydrophobicity of a surface is through the measurement of the "water contact angle", which is the angle measured through the water at the three-phase (liquid/substrate/air) point of contact. A high contact angle indicates a low level of adhesion with water, and surfaces with a water contact angle over 150° are considered to be "superhydrophobic". Certain plant leaves and insect wing membranes satisfy this criterion. Upon examination, many similarities have been shown to exist between the

ARTICLE

chemical and nano-structural properties of hydrophobic plant and insect cuticles, however, the outer surfaces of plant cuticles have been found to include a larger range of compounds, including aldehydes, ketones and fatty acids, whereas insect cuticle surfaces are predominantly comprised of long chain alkanes.

We have applied infrared microspectroscopy and imaging to the analysis of the spatially resolved chemical composition of the wing membrane of several insect species, including damselflies *Ischnura heterosticta* and *Xanthagrion erythroneurum*, dragonflies *Diplacodes bipunctata* and *Diplacodes melanopsis*, and the Clanger cicada *Psaltoda claripennis*.[9–10] The sensitivity of Fourier transform infrared (FT-IR) microspectroscopy to the varied functional groups making up the insect wing membrane made it an ideal technique for probing the chemical properties of these structures at the micron scale, while SEM was used to examine the nanoscale topography of these membranes. Infrared microanalysis was undertaken at two synchrotron beamlines—the Infrared Microspectroscopy (IRM) beamline at the Australian Synchrotron, which operates a conventional point mapping Fourier transform infrared (FT-IR) microscope, and the IRENI IR imaging beamline at the Synchrotron Radiation Center (SRC), Madison, Wisconsin. By coupling an FT-IR microscope to a synchrotron source, significant advantages could be gained with regard to the intensity of the focused beam for single point FT-IR microanalysis of samples areas of the order of $3–5\,\mu m^2$. Two-dimensional mapping of samples with this focused beam also allowed high spectral quality IR absorbance maps to be generated with diffraction limited spatial resolution, and this method was employed by the IRM beamline.[11] The IRENI beamline at SRC, however, was designed to enable the use of a Focal Plane Array (FPA) IR imaging detector of 128×128 detector pixels in conjunction with a high magnification $74\times$ microscope objective, which was made possible by the collection of twelve separate infrared beams from the SRC "ALADDIN" synchrotron storage ring.[12] Although the SRC ALADDIN

synchrotron ceased operation in 2014, the IRENI beamline enabled the high spatial resolution mapping of a range of materials and its success has led the planning of similar beamlines at other synchrotron facilities.

## FT-IR spectroscopy and imaging of dragonfly and damselfly wing membranes

Dragonfly and damselfly wings were obtained from two sources. Fresh wings of the species *D. bipunctata* and *I. heterosticta*, were obtained from suburban regions of Melbourne, Australia, while aged samples of *D. melanopsis* and *X. erythroneurum*, collected in the 1970s, were provided by Museum Victoria, Australia. Scanning electron microscopy (FeSEM–Supra 40VP, Carl Zeiss GmbH, Jena, Germany) of gold-coated wing membranes showed that the surfaces of the *Odonata* wings possess an outer layer of nanometre-scale structures that are randomly distributed across the

surface, as shown for the damselfly *I. heterosticta* in Figure 1A. While the overall pattern was found to be broadly similar between the four species, the size and separation of these structures was found to vary slightly between species. An FT-IR microanalysis of all four *Odonata* species wing membranes was conducted at the Australian Synchrotron IRM beamline, using a Bruker Hyperion 2000 IR microscope and V80v FT-IR spectrometer. Small sections of wing membrane, approximately $5 \times 5\,mm^2$, were mounted in a metal frame to support the edge of the sample and avoid movement of the delicate membrane during analysis. Spectra produced for all samples were consistent with the known composition of the insect cuticle (Figure 1B), with strong Amide I ($1610–1695\,cm^{-1}$) and Amide II ($1480–1575\,cm^{-1}$) absorption bands from the amide and amine groups of protein and chitin, as was a small C=O ester peak at $1735\,cm^{-1}$, CH_2 and CH_3 stretching peaks (νCH_2 and νCH_3, $2840–3000\,cm^{-1}$) from protein, chitin, alkanes
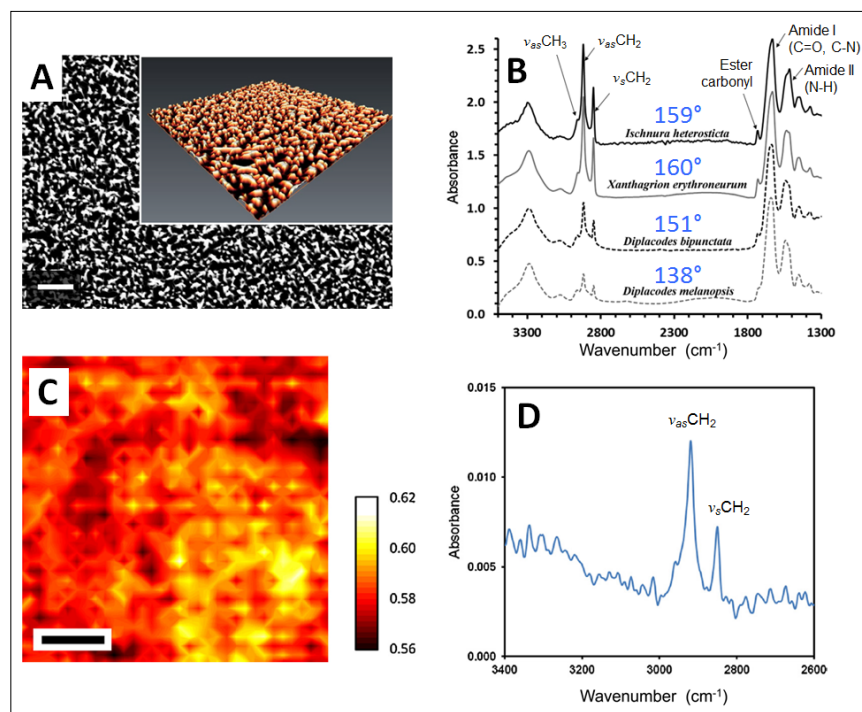
Figure 1. Topographic and chemical properties of damselfly and dragonfly wings. (A) Scanning electron micrograph in 2D and 3D projection (inset) of damselfly *Ischnura heterosticta* wing (scale bar = 1 µm). (B) IR absorbance spectra, averaged from multiple locations, of wings from four *Odonata* species, indicating key functional groups. Water contact angle for each species' wing is shown in blue. (C) $\nu_{as}CH_2$ integrated absorbance map of the *I. heterosticta* wing membrane (scale bar = 20 µm). (D) Spectral difference between high CH_2 absorbance and low CH_2 absorbance areas of *I. heterosticta* wings. Reproduced and adapted from Reference 9.

and fatty acids, and broad overlying O–H and N–H stretching peaks obtained between $3200\,cm^{-1}$ and $3400\,cm^{-1}$. The most notable difference between the four species was the strength of the νCH peaks, in particular the symmetric and antisymmetric νCH_2 peaks, with both damselfly species showing stronger νCH_2 absorption than either of the dragonfly species. Two-dimensional spectral mapping of small areas of each species' wings was performed using a $5 \times 5\,\mu m^2$ microscope aperture for $3\,\mu m$ steps in both the x and y directions over a total area of $100 \times 100\,\mu m^2$. Figure 1C shows a plot of the integrated area of the antisymmetric $\nu_{as}CH_2$ peak between $2913\,cm^{-1}$ and $2931\,cm^{-1}$ across the wing membrane of the *I. heterosticta* damselfly, showing the heterogeneous nature of this distribution. Spectral subtraction of lower intensity νCH spectra from this 2D data set (black areas in Figure 1C) from higher νCH spectra (yellow areas in Figure 1C), confirmed that the main contribution to the higher νCH areas was from symmetric and antisymmetric νCH_2 stretching (Figure 1D), indicating a heterogeneous distribution of long chain hydrocarbons such as waxes across the wing membrane. This is consistent with observations reported elsewhere, in which solvent extraction followed by the gas chromatography-mass spectrometry (GC-MS) analysis of wing membranes from the dragonfly *Hemicordulia tau* indicated the dominance of long chain alkanes of chain length from C_{10} to C_{34}, with a smaller contribution (7%) being obtained from palmitic acid.[8] Water contact angle measurements were made of wing membranes from each of the four species of dragonfly and damselfly studied, and the observed angles are shown against the IR absorbance spectra for each species in Figure 1B. These show a clear relationship between the long chain wax concentration, as indicated by the strength of the νCH_2 peaks, and the water contact angle, showing that the species with higher CH_2 absorbance show the greatest hydrophobicity, indicating a role for the chemical composition as well as the surface nanostructuring in promoting the superhydrophobic property of these insects' wings.
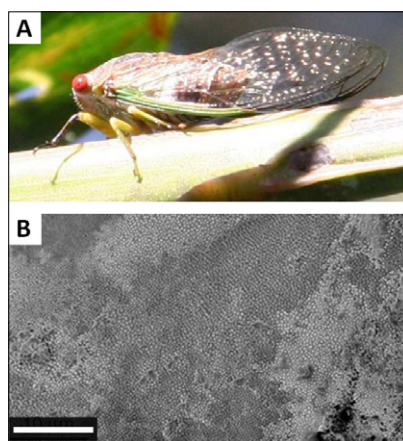
Figure 2. (A) Cicada *Psaltoda claripennis*. (B) SEM image of wing membrane surface of *Psaltoda claripennis* cicada (scale bar = $10\,\mu m$). Reproduced with permission of the International Union of Crystallography, from Reference 10.

FT-IR spectroscopy and imaging of cicada wing membranes

The native Australian cicada *Psaltoda claripennis* is shown in Figure 2A, examples of which were collected from Brisbane parkland areas. Sections of the wing membrane (approximately $5\,\mu m$ in thickness) were then cut into squares approximately $5 \times 5\,mm^2$ and rinsed with Milli-Q H_2O (resistivity of $18.2\,M\Omega\,cm^{-1}$) before being used for microanalysis.[6] SEM of gold-coated wing membranes showed the presence of a highly regular pattern of "nanopillars" across the wing surface (Figure 2B), with an additional micron-scale texture also observed. It is these nanopillar structures that have been shown to be responsible for the bactericidal properties of these cicada wings, with the structures appearing to penetrate the membrane of bacteria that became attached to the surface. FT-IR spectroscopic imaging of the cicada wing membranes was conducted at the SRC IRENI beamline, Madison, Wisconsin.[10] Wing samples were mounted into the same metal support frame used for the *Odonata* wings, and 64×64 pixel IR image frames were captured, each covering an area of $34.5 \times 34.5\,\mu m^2$. IR absorbance spectra of the cicada wings were found to be broadly similar to those obtained for the *Odonata* wings, showing the presence of spec-

tral peaks attributable to protein, chitin, alkanes and fatty acids. Multiple image frames were tiled together to produce IR absorption images covering a larger area. Figure 3A–F shows IR absorption maps of two regions of wing, one covered by a 3×3 frame map (A, C and E) and one covered by a 4×1 frame map (B, D and F). In each case, an image of the Amide II distribution (integrated from $1483\,cm^{-1}$ to $1588\,cm^{-1}$) and $\nu_{as}CH_2$ distribution ($2913–2931\,cm^{-1}$) is shown. A third image is a Red:Green:Blue (RGB) composite in which the red and green channels are combined from the $\nu_{as}CH_2$ map, with the blue channel showing the Amide II. These images indicate that the Amide II peak shows a small amount of variation over the two image areas (Figure 3A and B) probably due to differences in wing membrane thickness, whereas the $\nu_{as}CH_2$ images (Figure 3C and D) show punctate distribution, with distinct features of a few microns in size seen as red spots in the $\nu_{as}CH_2$ map. These show up clearly as yellow spots in the combined RGB images (Figure 3E and F), indicating localised high concentrations of long chain hydrocarbons. Furthermore, a larger scale patterning or texture can be discerned over the areas of wing imaged, with CH_2 "points" appearing to cluster into certain areas, while other areas show fewer spots. Figure 3G shows the CH stretch region ($2800–3150\,cm^{-1}$) of selected spectra from a high CH_2 "spot" in Figure 3C (red trace) and a low CH_2 area (black trace). The spectral subtraction of these traces is shown in Figure 3H, confirming that the high CH features in the IR images are due primarily to long chain aliphatic hydrocarbons, since only symmetric and antisymmetric νCH_2 stretching peaks, along with a weaker C–H bending peak around $1470\,cm^{-1}$ (not shown), were observed in the subtracted spectra.

In the case of the cicada wing, evidence could be seen of a hierarchical distribution of the hydrophobic wing surface coating. This combination of micron scale hydrocarbon features, arranged in patterns on the scale of tens of microns, may contribute to the high hydrophobicity of the cicada wing, which for *P. claripennis* has been shown

ARTICLE
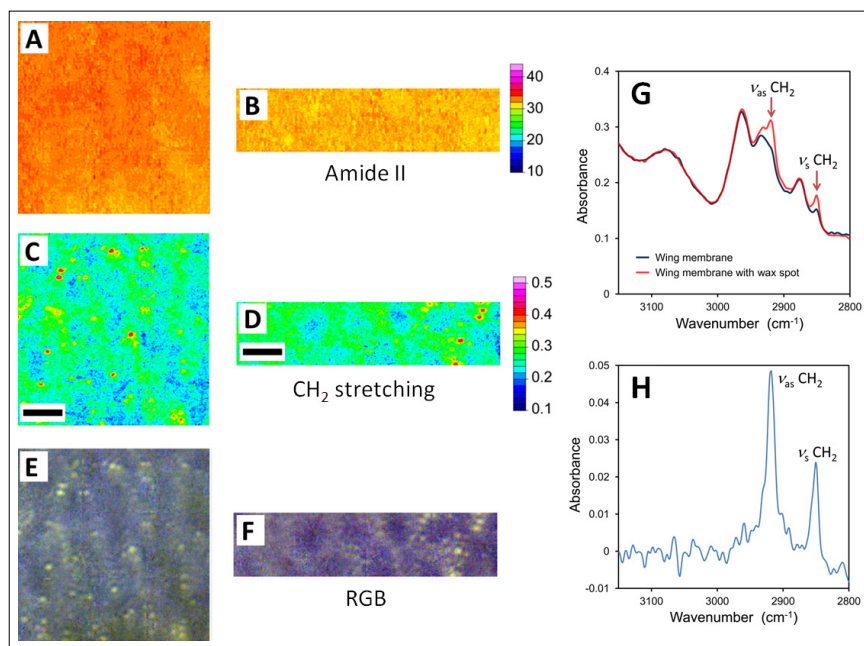
Figure 3. IR absorbance maps and IR absorbance spectra of the *Psaltoda claripennis* cicada wing membrane. (A, B) Amide II integrated absorbance maps (integrated area 1483–1588 cm^{-1}) and (C, D) ν_{as}CH$_2$ integrated absorbance maps (integrated area 2913–2931 cm^{-1}) (scale bars = 20 μm). (E, F) RGB composite images of same data sets, showing the blended presence of Amide II (B) and ν_{as}CH$_2$, (R+G) resulting in the aliphatic hydrocarbons showing as yellow, with the combination of protein and chitin showing as blue. (G) Selected IR absorbance spectra from high (red) and low (black) ν_{as}CH$_2$ regions of the IR absorbance maps. (H) Spectral subtraction showing the overall difference between the high and low ν_{as}CH$_2$ spectra is due only to symmetric and antisymmetric CH$_2$ stretching vibrations. Reproduced with permission of the International Union of Crystallography, from Reference 10.

to have a water contact angle of greater than 150° and is therefore considered to be superhydrophobic.

Conclusion

Insect wings possess some remarkable properties, enabling them to thrive in challenging environments. Often, a combination of nano- and micro-structured topography, with chemical heterogeneity on the micron scale, provides these structures with efficient superhydrophobic, self-cleaning and antibacterial capabilities. Their complex surfaces are providing inspiration for the design of novel coatings and surface structures that can mimic these beneficial properties. High spatial resolution FT-IR spectroscopy and imaging, when combined with other techniques such as SEM and GC-MS, provide unique insights into the complex chemical patterning that contributes to this functionality. Further developments in FT-IR imaging, such as 3D infrared tomography and scanning near-field nano spectroscopy[13,14] have the potential to add a further dimension to the chemical and physical information that is enabling us to obtain a greater understanding of these natural surfaces. These techniques can also continue to be applied to the study of man-made material surfaces that attempt to emulate the properties of their biological templates.

References

1. S.H. Nguyen, H.K. Webb, P.J. Mahon, R.J. Crawford and E.P. Ivanova, "Natural insect and plant micro-/nanostructured surfaces: an excellent selection of valuable templates with superhydrophobic and self-cleaning properties", *Molecules* **19,** 13614 (2014). doi: http://dx.doi.org/10.3390/molecules190913614
2. W. Barthlott and C. Neinhuis, "Purity of the sacred lotus, or escape from contamination in biological surfaces", *Planta* **202,** 1 (1997). doi: http://dx.doi.org/10.1007/s004250050096
3. T. Wagner, C. Neinhuis and W. Barthlott, "Wettability and contaminability of insect wings as a function of their surface sculptures", *Acta Zool*. **77,** 213 (1996). doi: http://dx.doi.org/10.1111/j.1463-6395.1996.tb01265.x
4. J. Hasan, H.K. Webb, V.K. Truong, G.S. Watson, J.A. Watson, M.J. Tobin, G. Gervinskas, S. Juodkazis, J.Y. Wang, R.J. Crawford and E.P. Ivanova, "Spatial variations and temporal metastability of the self-cleaning and superhydrophobic properties of damselfly wings", *Langmuir* **28,** 17404 (2012). doi: http://dx.doi.org/10.1021/la303560w
5. M. Sun, G.S. Watson, Y. Zheng, J.A. Watson and A. Liang, "Wetting properties on nanostructured surfaces of cicada wings", *J. Exp. Biol*. **212,** 3148 (2009). doi: http://dx.doi.org/10.1242/jeb.033373
6. E.P. Ivanova, J. Hasan, H.K. Webb, V.K. Truong, G.S. Watson, J.A. Watson, V.A. Baulin, S. Pogodin, J.Y. Wang, M.J. Tobin, C. Löbbe and R.J. Crawford, "Natural bactericidal surfaces: Mechanical rupture of *Pseudomonas aeruginosa* cells by cicada wing", *Small* **8,** 2489 (2012). doi: http://dx.doi.org/10.1002/smll.201200528
7. Y. Yoon, D. Kim and J.-B. Lee, "Hierarchical micro/nano structures for super-hydrophobic surfaces and super-lyophobic surface against liquid metal", *Micro Nano Syst. Lett.* **2,** 1 (2014). doi: http://dx.doi.org/10.1186/s40486-014-0003-x
8. S.H. Nguyen, H.K. Webb, J. Hasan, M.J. Tobin, R.J. Crawford and E.P. Ivanova, "Dual role of outer epicuticular lipids in determining the wettability of dragonfly wings", *Colloid. Surface. B* **106,** 126 (2013). doi: http://dx.doi.org/10.1016/j.colsurfb.2013.01.042
9. S.H. Nguyen, H.K. Webb, J. Hasan, M.J. Tobin, D.E. Mainwaring, P.J. Mahon, R. Marchant, R.J Crawford and E.P. Ivanova, "Wing wettability of *Odonata* species as a function of quantity of epicuticular waxes", *Vibr. Spectrosc.* **75,** 173 (2014). doi: http://dx.doi.org/10.1016/j.vibspec.2014.07.006
10. M.J. Tobin, L. Puskar, J. Hasan, H.K. Webb, C.J. Hirschmugl, M.J. Nasse, G. Gervinskas, S. Juodkazis, G.S. Watson, J.A. Watson, R.J. Crawford and E.P. Ivanova, "High-spatial-resolution mapping of superhydrophobic cicada wing surface chemistry using infrared microspectroscopy and infrared imaging at two synchrotron beamlines", *J. Synchrotron Radiat.* **20,** 482 (2013). doi: http://dx.doi.org/10.1107/S0909049513004056
11. P. Heraud, S. Caine, N.Campanale, T. Karnezis, D. McNaughton, B.R. Wood, M.J. Tobin and C.C.A. Bernard, *Neuroimage* **49,** 1180 (2010). doi: http://dx.doi.org/10.1016/j.neuroimage.2009.09.053
12. M.J. Nasse, M.J. Walsh, E.C. Mattson, R. Reininger, A. Kajdacsy-Balla, V. Macias, R. Bhargava and C.J. Hirschmugl, *Nat. Methods* **8,** 413 (2011). doi: http://dx.doi.org/10.1038/nmeth.1585
13. M.C. Martin, C. Dabat-Blondeau, M. Unger, J. Sedlmair, D.Y. Parkinson, H.A. Bechtel, B. Illman, J.M. Castro, M. Keiluweit, D. Buschke, B. Ogle, M.J. Nasse and C.J. Hirschmugl, "3D spectral imaging with synchrotron Fourier transform infrared spectro-microtomography", *Nat. Methods* **10,** 861 (2013). doi: http://dx.doi.org/10.1038/nmeth.2596
14. H.A. Bechtel, E.A. Muller, R.L. Olmon, M.C. Martin and M.B. Raschke, "Ultrabroadband infrared nanospectroscopic imaging", *Proc. Natl. Acad. Sci. USA* **111,** 7191 (2014). doi: http://dx.doi.org/10.1073/pnas.1400502111